JACS
JOURNAL OF THE AMERICAN CHEMICAL SOCIETY
Article
pubs.acs.org/JACS

A Structure–Function Relationship for the Optical Modulation of Phenyl Boronic Acid-Grafted, Polyethylene Glycol-Wrapped Single-Walled Carbon Nanotubes

Bin Mu,[‡] Thomas P. McNicholas,[‡] Jingqing Zhang,[‡] Andrew J. Hilmer,[‡] Zhong Jin,[‡] Nigel F. Reuel,[‡] Jong-Ho Kim,[§] Kyungsuk Yum,[‡] and Michael S. Strano*[,‡]

[‡]Department of Chemical Engineering, Massachusetts Institute of Technology, Cambridge, Massachusetts 02139, United States
[§]Department of Chemical Engineering, Hanyang University, Ansan 426-791, Republic of Korea

Supporting Information

ABSTRACT: Phenyl boronic acids (**PBA**) are important binding ligands to pendant diols useful for saccharide recognition. The aromatic ring can also function to anchor an otherwise hydrophilic polymer backbone to the surface of hydrophobic graphene or carbon nanotube. In this work, we demonstrate both functions using a homologous series of seven phenyl boronic acids conjugated to a polyethylene glycol, eight-membered, branched polymer (**PPEG8**) that allows aqueous dispersion of single-walled carbon nanotubes (SWNT) and quenching of the near-infrared fluorescence in response to saccharide binding. We compare the 2-carboxyphenylboronic acid (**2CPBA**); 3-carboxy- (**3CPBA**) and 4-carboxy- (**4CPBA**) phenylboronic acids; *N*-(4-phenylboronic)succinamic acid (**4SCPBA**); 5-bromo-3-carboxy- (**5B3CPBA**), 3-carboxy-5-fluoro- (**5F3CPBA**), and 3-carboxy-5-nitro- (**5N3CPBA**) phenylboronic acids, demonstrating a clear link between SWNT photoluminescence quantum yield and boronic acid structure. Surprisingly, quantum yield decreases systematically with both the location of the BA functionality and the inclusion of electron-withdrawing or -donating substituents on the phenyl ring. For three structural isomers (**2CPBA**, **3CPBA**, and **4CPBA**), the highest quantum yields were measured for para-substituted PBA (**4CPBA**), much higher than ortho- (**2CPBA**) and meta- (**3CPBA**) substituted PBA, indicating the first such dependence on molecular structure. Electron-withdrawing substituents such as nitro groups on the phenyl ring cause higher quantum yield, while electron-donating groups such as amides and alkyl groups cause a decrease. The solvatochromic shift of up to 10.3 meV was used for each case to estimate polymer surface coverage on an areal basis using a linear dielectric model. Saccharide recognition using the nIR photoluminescence of SWNT is demonstrated, including selectivity toward pentoses such as arabinose, ribose, and xylose to the exclusion of the expected fructose, which has a high selectivity on PBA due to the formation of a tridentate complex between fructose and PBA. This study is the first to conclusively link molecular structure of an adsorbed phase to SWNT optical properties and modulation in a systematic manner.

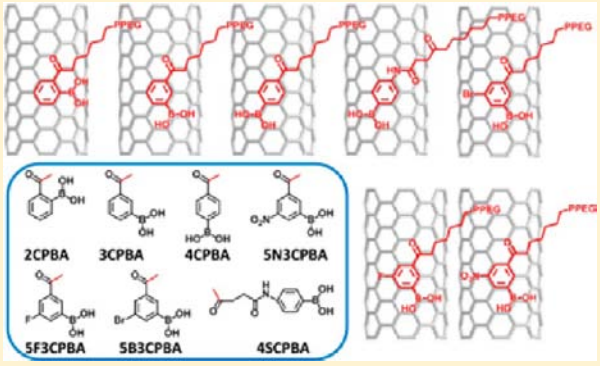

INTRODUCTION

The interaction between a phenylboronic acid (PBA) and a diol is known to be one of the strongest single-pair reversible functional group interactions in aqueous media.[1,2] Such interactions involve a well-studied, multicomponent equilibrium that involves proton dissociation from the acid, resulting in equilibrium between the trigonal (neutral boronic acid) and tetrahedral deprotonated (negatively charged boronate ion) forms of known acidity K_a. In the presence of diols, both (trigonal and tetrahedral) forms can bind with 1,2- or 1,3-diols to form a diol–phenylboronate complex with either five- or six-membered ring systems, respectively. Boronate complexes have increased acidity compared to the starting boronic acid. Thus, the 1,2- or 1,3-diols present on saccharides provides an ideal scaffold for these interactions and has led to the development of boronic acid-based sensors for saccharides.[1−3]

Semiconducting single-walled carbon nanotubes (SWNTs) are excellent candidates for fluorescent sensors due to their stable fluorescence at near-infrared (nIR) wavelengths without photobleaching.[4,5] Our laboratory and others have shown that SWNT emission is affected by changes in the local dielectric environment (solvatochromism),[6,7] electron transfer (doping),[8,9] or fluorescent quenching.[10] These concepts can be utilized to create sensors for glucose,[11−13] nitric oxide,[9] nitroaromatics,[14] hydrogen peroxide,[15] and proteins.[10,16] Thus, design and synthesis of wrappings with specific recognition groups are important in constructing novel fluorescent sensors. Over the past few decades, polymers have been utilized for noncovalent dispersion of SWNT in various solvents.[17,18] This dispersion is enabled by wrapping or

Received: July 19, 2012
Published: September 14, 2012

dx.doi.org/10.1021/ja307085h | *J. Am. Chem. Soc.* 2012, 134, 17620−17627

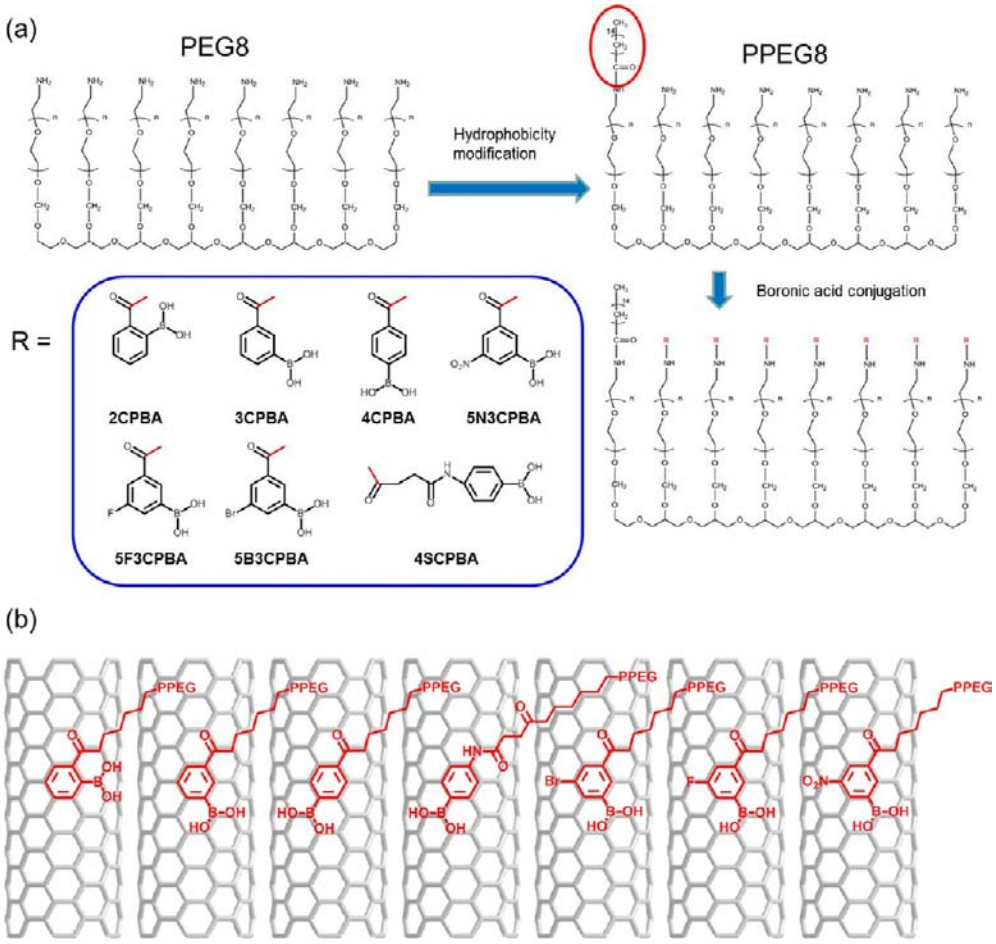

Figure 1. (a) Synthesis scheme of a series of PBA-conjugated amphiphilic PEG polymers presents two steps including hydrophobicity modification of PEG8 and boronic acid conjugation. (b) Proposed wrapping geometry of different PBAs on a SWNT (From left to right: 2CPBA-PPEG8, 3CPBA-PPEG8, 4CPBA-PPEG8, 4SCPBA-PPEG8, 5B3CPBA-PPEG8, 5F3CPBA-PPEG8, and 5N3CPBA-PPEG8). The highest photoluminescence quantum yield was observed for para-substituted PBA (4CPBA), much higher than ortho (2CPBA)- and meta (3CPBA)-substituted PBA.

adsorbing amphiphilic polymers around the SWNT, using for example a $\pi-\pi$ stacking[19] arrangement to secure an otherwise water-soluble polymer. Electrostatic interactions[20] and hydrogen bonding[21] allow for stabilization of the nanotubes in solution. Understanding the intermolecular interactions between the polymer-adsorbed phase and SWNT surface can improve and augment the molecular recognition necessary to create fluorescent sensors. However, our knowledge about the effect of polymer structure on the fluorescence of SWNTs requires further study.[22]

Boronic acid polymers have proven valuable in a variety of biomedical applications.[23,24] Applications include lipase inhibition,[25] HIV inhibition,[26] controlled drug delivery,[27] and boron neutron capture therapy,[28] as well as glycan or saccharide detection.[29] Sugar detection with boronic acid-based systems generally relies on either optical or conductivity changes upon binding of a sugar with a boronic acid moiety. For instance, Wang and co-workers demonstrated a fluorescent imprinted polymer with boronic acid groups, which showed an increase in fluorescence intensity on the addition of D-fructose.[30] Freud et al. reported the potentiometric detection of saccharides using a polyaniline boronic acid-based system.[31]

In this work, we synthesize a homologous series of seven phenyl boronic acid conjugated polyethylene glycol 8-membered branched polymers (**PPEG8**), using 2-carboxyphenylboronic acid (**2CPBA**), 3-carboxyphenylboronic acid (**3CPBA**), 4-carboxyphenylboronic acid (**4CPBA**), *N*-(4-phenylboronic)-succinamic acid (**4SCPBA**), 5-bromo-3-carboxyphenylboronic acid (**5B3CPBA**), 3-carboxy-5-fluorophenylboronic acid (**5F3CPBA**), and 3-carboxy-5-nitrophenylboronic acid (**5N3CPBA**). Figure 1 outlines the structures considered in this work. We evaluated their ability to disperse SWNTs in aqueous suspension, the relative n-IR fluorescence quantum yield and solvatochromic shift. Saccharide recognition indicates that pentoses such as arabinose, ribose, and xylose cause larger fluorescence quenching responses compared with those of other saccharides. Thus, a novel signal transfer mechanism can be proposed to manipulate the selectivity of saccharide recognition. This study is the first to conclusively link molecular structure to SWNT optical properties in a systematic manner and can therefore guide the synthesis of optical switches and sensors based on SWNT.

■ RESULTS AND DISCUSSION

PEG polymers have been studied for many years as effective drug delivery reagents and for *in vivo* testing due to their excellent biocompatibility.[32] In this work, an amine functionalized 8-arm PEG polymer was selected as the backbone of wrapping reagent to disperse SWNT. Furthermore, palmitoyl chloride was used to modify one of the amine groups on PEG8 so that the hydrophobic alkyl groups of the polymer (PPEG8) can bind with the

dx.doi.org/10.1021/ja307085h | J. Am. Chem. Soc. 2012, 134, 17620−17627

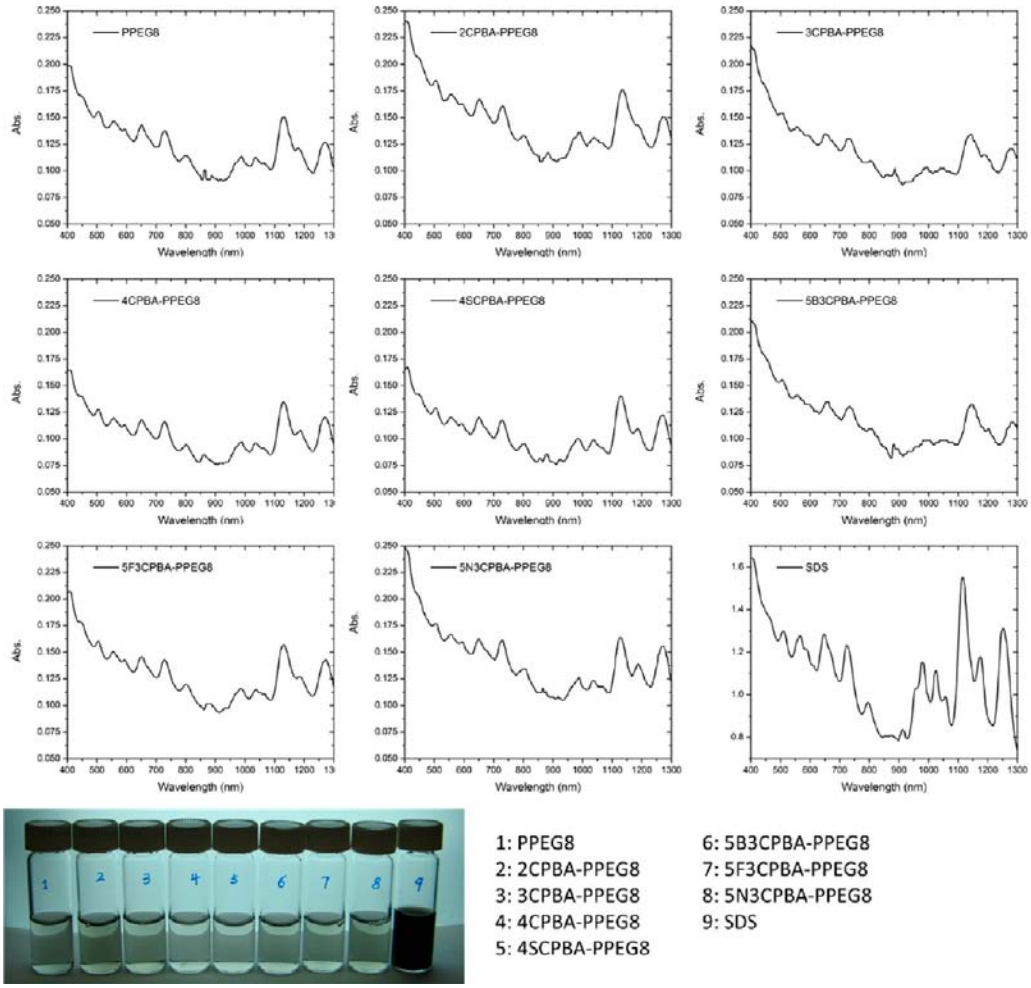

Figure 2. UV−vis−nIR absorption spectrum of SWNTs wrapped by different wrapping agents. Ten milligrams of SWNTs was dispersed in 30 mL of distilled water using 40 mg of polymers, or at 1% SDS concentration. Samples were sonicated in a cold water bath with a 5 mm probe tip for 40 min at a power of 25 W, followed by ultracentrifugation for 4 h at 30,000 rpm (~164,100*g*). All polymers appear to disperse SWNT comparably, with a yield ~10−15% compared to that dispersed using SDS.

Table 1. Summary of Solvatochromism Analysis, Surface Coverage Calculation, Dispersion Efficiency, and Quantum Yield of SWNTs Dispersed by PBA-PPEG8 Polymers[a]

reagents	slope (E_{11}) [eV^3 nm^4]	slope (E_{22}) [eV^3 nm^4]	ratio (E_{22}/E_{11})	surface coverage (%)	relative dispersion efficiency (%)	relative quantum yield (%)
SDS	0.050	0.188	3.76	100	100	–
PPEG8	0.054	0.195	3.61	69	11	100
2CPBA-PPEG8	–	–	–		9	10
3CPBA-PPEG8	–	–	–		13	7
4CPBA-PPEG8	0.061	0.198	3.25	72	11	88
4SCPBA-PPEG8	0.058	0.199	3.43	70	9	50
5B3CPBA-PPEG8	–	–	–		13	29
5F3CPBA-PPEG8	–	–	–		11	18
5N3CPBA-PPEG8	0.056	0.201	3.59	69	10	66

[a]Slopes of solvatochromism analysis are obtained by fitting the data into a straight line as shown in Figure 4. Surface coverage of SDS-SWNT of 100% is based on the two assumptions: (1) the surface packing density of SDS is 1.7 molecules/nm^2 according to the reported experimental results;[40] (2) each SDS molecule occupies a surface area of about 0.59 nm^2 reported by Almgren and Swarup[41] due to the consideration of different SDS configurations in the presence of SWNTs.[42,43] Relative dispersion efficiency is calculated on the basis of optical density at 632 nm in UV−vis−nIR absorption spectra. Relative quantum yield is calculated on the basis of peak intensity of SWNT (9, 4) on the nIR fluorescence spectrum.

hydrophobic surface of SWNTs, while the rest of amine groups on PPEG8 will be used to conjugate different PBAs as the recognition groups of saccharides. Eight polymers including PPEG8 and seven others with different PBA moieties were synthesized and examined as amphiphillic polymers for SWNT dispersion (Figure 1). The dispersion procedure was identical for all the polymers, and no SWNT precipitation was observed for at least three weeks. The UV−vis−nIR absorption spectra of all PBA-PPEG8 polymer−SWNTs complexes (**1** to **8**) were compared with that of SDS-SWNTs (**9**) (Figure 2).

dx.doi.org/10.1021/ja307085h | *J. Am. Chem. Soc.* 2012, 134, 17620−17627

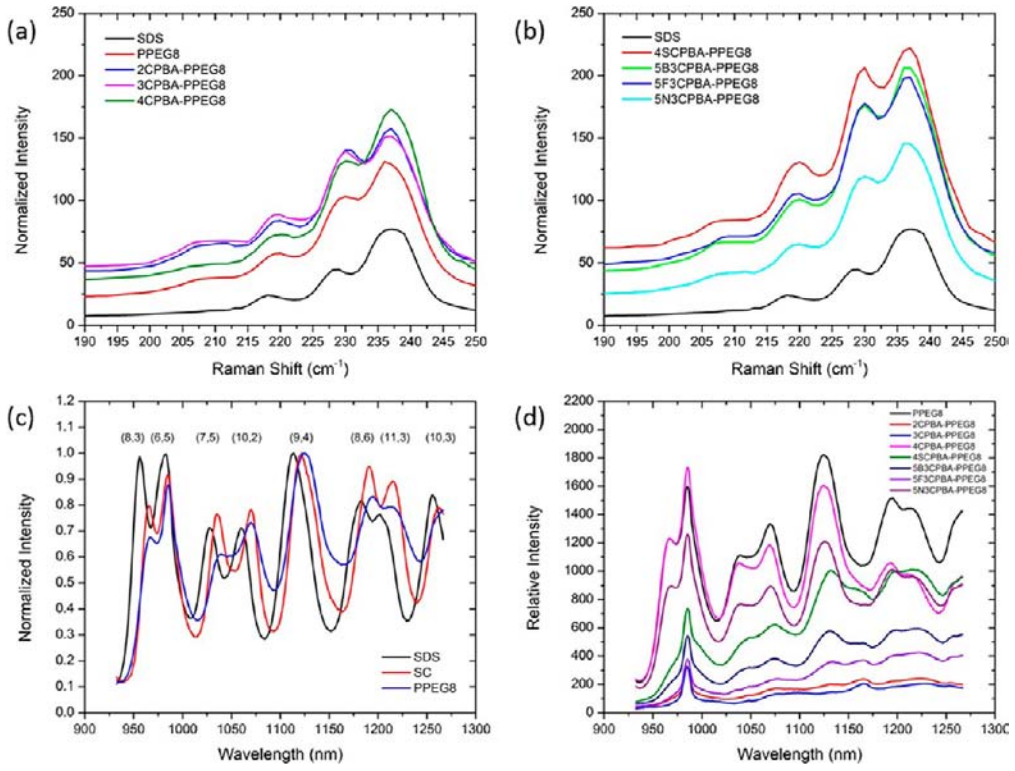

Figure 3. (a,b) Raman spectra showing no difference on Raman shift for different wrapping agents; (c) nIR fluorescence comparison of Unidym SWNTs dispersed in SDS, SC, and PPEG8 showing an apparent wavelength shift of SWNT emission, where the red-shift of the PPEG8-SWNT emission wavelength is noted at up to 10.3 and 7.8 meV compared to those of SDS-SWNT and SC-SWNT; (d) nIR fluorescence of PBA-PPEG8 polymer–SWNTs complexes showing different quenching ability compared with those of PPEG8-SWNTs. Specifically, among three structural isomers (2CPBA, 3CPBA, and 4CPBA), the highest quantum yield was measured for para-substituted PBA (4CPBA, −12%), much higher than those of ortho (2CPBA, −90%)- and meta (3CPBA, −93%)-substituted PBA. In addition, electron-withdrawing substituents such as a nitro group on the phenyl ring cause higher quantum yield (5N3CPBA, −34% vs 3CPBA, −93%), while electron-donating groups such as amides and alkyl groups decrease the quantum yield (4SCPBA, −50% vs 4CPBA, −12%).

All polymer–SWNT complexes had some fraction that remained after decanting following the ultracentrifugation process and demonstrated similar dispersion yields, though with concentrations lower than that of SDS-SWNTs with ranges between 10% to 15% of the case of SDS (Table 1). Relative dispersion efficiency is calculated on the basis of the optical density at 632 nm on UV–vis–nIR absorption spectrum.

Studying the interaction of aromatic compounds with SWNTs is of particular interest not only because it is a well-known method to noncovalently modify the surface of SWNTs,[33] but also it provides a fundamental theoretical and systematic understanding toward the design of novel sensors based on SWNTs.[34] Recent simulation results based on density-functional theory (DFT)[35,36] reveals that physisorption through $\pi-\pi$ binding dominates the adsorption mechanism; however, substitutional groups give rise to local electronic polarization and to shifts in vibrational lines due to small charge transfer, which also play important roles in the interaction. In this work, 7 PBAs with different substitutional groups or isomers lead to different binding energies on SWNTs,[36] and are therefore expected to produce changes in the photoluminescence due to charge transfer,[33,37] in which an electron donor–acceptor complex is formed between SWNTs and aromatic compounds, resulting in leveling the redox potential of different SWNT species. The radial breathing mode (RBM) frequencies in the Raman spectra appear invariant to changes in the boronic acid position and other ring substitutions (Figure 3a,b).

The nIR fluorescence spectra of PPEG8-SWNTs excited at 785 nm was compared with SDS-SWNTs and SC-SWNTs, revealing wavelength shifts and intensity changes likely due to differences in polymer wrapping (Figure 3c). Compared to the fluorescence of SDS-SWNTs, the wavelength of SC-SWNTs and PPEG8-SWNTs is red-shifted up to 2.5 and 10.3 meV, respectively. Such solvatochromic shifts of SWNTs indicated varied dielectric environments around SWNTs.[6] SC provides a lower surface coverage compared to tight packing by SDS,[6,38] yielding lower photoluminescence energies and a red-shift, while the sparse hydrophobic interaction of SWNT with the alky group of PPEG8 polymer allows water molecules close to the SWNT surface, resulting in further red-shifts. Furthermore, nIR fluorescence spectra of PBA-PPEG8 polymers present varied quenching compared to that of PPEG8 (Figure 3d), demonstrating the effect of different substitute groups of PBA on photoluminescence of SWNTs. The reactive quantum yield is calculated on the basis of the peak intensity of SWNT (9, 4) on nIR fluorescence spectrum normalized with absorbance (Table 1). Compared to that of PPEG8, the quantum yields of SWNTs dispersed by all PBA-PPEG8 decrease to different levels, including 2CPBA-PPEG8 (−90%), 3CPBA-PPEG8 (−93%), 4CPBA-PPEG8 (−12%), 4SCPBA-PPEG8 (−50%), 5B3CPBA-PPEG8 (−71%), 5F3CPBA-PPEG8 (−82%), and 5N3CPBA-PPEG8 (−34%). Among three structural isomers (2CPBA, 3CPBA, and 4CPBA), comparison of the results of ortho-, meta-, and para-substituted PBA indicated that variations in the conformation have important effects on the quantum yield of SWNTs stemming from differences of the dihedral angle between

dx.doi.org/10.1021/ja307085h | J. Am. Chem. Soc. 2012, 134, 17620–17627

aromatic ring and the surface of SWNTs, which is consistent with the results from molecular dynamics studies.[39]

A pristine SWNT has no net dipole moment, but is highly polarizable. Thus, a dipolar solvent or a dipolar molecule near the SWNT surface can induce a dipole moment and cause a shift in the optical transition energies (E_{ii}), which are proportional to the difference in SWNT polarizability, $\Delta\alpha_{ii}$, between the excited and ground states for the E_{ii} transitions. By measuring photoluminescence excitation−emission profiles, the E_{ii} shift of individual SWNT can be probed. Here, excitation−emission profiles of SWNTs dispersed by PPEG8, 4CPBA-PPEG8, 4SCPBA-PPEG8, and 5N3CPBA-PPEG8 were compared to that of SDS (Figure 4). By using a previously proposed model,[6] the relationship between $(E_{ii}^{\text{air}})^2(E_{ii}^{\text{air}} - E_{ii}^{\text{solvent}})$ and d^{-4} was plotted in Figure 4, in which the values of E_{ii}^{air} were calculated according to the fitted model parameters, and the relationship between the local dielectric constant (ε) and the fraction of SWNT surface area covered by polymer (α) is given by:

$$(E_{ii})^2 \Delta E_{ii} = -Lk\left[\frac{2(\varepsilon - 1)}{2\varepsilon + 1} - \frac{2(n^2 - 1)}{2n^2 + 1}\right]\left(\frac{1}{R^4}\right) = \frac{c}{R^4} \quad (1)$$

$$\varepsilon = \alpha\varepsilon_{\text{media}} + (1 - \alpha)\varepsilon_{\text{water}} \quad (2)$$

where L is a fluctuation factor, k a constant, n the refractive index, and $\varepsilon_{\text{water}} = 88.1$, $\varepsilon_{\text{SDS}} = 31$, $\varepsilon_{\text{PEG8}} = 2.5$ represent the dielectric constants of water, SDS, and PEG8, respectively. Similar to the SDS case, both transitions for all examined PBA-PPEG8-SWNTs demonstrate linear scaling, while E_{22} has increased data scattering than E_{11} data due to lower measurement resolution. The slopes are 0.050 and 0.188 eV^3 nm^4 for the E_{11} and E_{22} of SDS-SWNT, which are the same as previously reported. The magnitudes of the E_{11} slope and the E_{22} slope of PBA-PPEG8-SWNTs increase (relative to SDS-SWNT), as expected due to the lower surface coverage and therefore increased dielectric constant, causing a larger PL red-shift. The ratio of the slopes of E_{22}/E_{11} is lower than for the SDS case, highlighting the fact that E_{22} is less affected by the surrounding medium, as we have shown previously.[6] In addition, if we assume a reference surface coverage of SWNTs dispersed by SDS as 100%, the calculated surface coverage of SWNTs dispersed by different PBA-PPEG8 varies from 65% to 75% (Table 1). This smaller surface coverage is consistent with the longer hydrocarbon chain used here resulting in "inaccessible" surface area excluded by the media due to steric effects. The estimate of 100% surface coverage of SDS-SWNT is based on the two assumptions: (1) the surface packing density of SDS is 1.7 molecules/nm^2, according to the reported experimental results;[40] and (2) each SDS molecule occupies a surface area of about 0.59 nm^2, reported by Almgren and Swarup,[41] due to the consideration of different SDS configurations in the presence of SWNTs.[42,43]

Boronic acids can bind diol moieties with high affinity through reversible boronate formation. Alizarin Red S (ARS) is a fluorophore frequently employed to determine the PBA concentration and to monitor saccharide binding events.[44] ARS itself is nonfluorescent, and PBA can bind to the catechol diol of ARS to remove the active protons of hydroxyanthraquinones, causing a visible fluorescence (Figure 5). However, saccharides can bind to PBA as well. Thus, the competitive equilibrium between ARS and an ARS−PBA complex is perturbed upon saccharide addition, resulting in a fluorescence intensity change that corresponds directly to the saccharide binding affinity. As shown in Figure 5, all

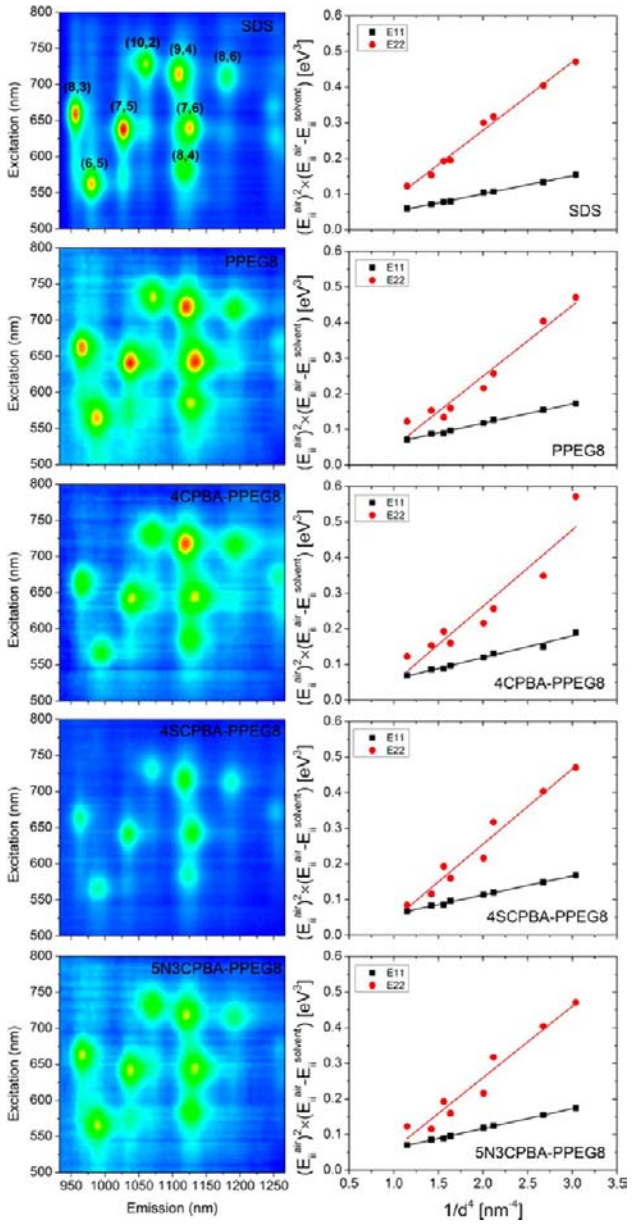

Figure 4. Excitation−emission profile of PBA-PPEG8-SWNT complexes. Left: contour plot of fluorescence intensity versus excitation and emission wavelengths for a sample of SWNTs suspended in different wrapping agents. Right: by using a previously proposed model,[6] the relationship between the optical transition energies and the diameter of SWNT ($(E_{ii}^{\text{air}})^2(E_{ii}^{\text{air}} - E_{ii}^{\text{solvent}})$ vs d^{-4}) was plotted and fitted into a straight line, in which the values of E_{ii}^{air} were calculated according to the model parameters.

PBA-PPEG8 polymers can cause an apparent fluorescence from the binding between PBA and ARS, which confirms that boronic acid molecules were successfully conjugated to PPEG8 polymers. Furthermore, equal amounts of different sugar molecules were added to test the binding selectivity (Figure 5b). Our results demonstrate that the synthesized PBA-PPEG8 polymers all have the same saccharide binding selectivity with fructose > galactose > mannose > glucose > sucrose. In addition, 5N3CPBA-PPEG8 presented the highest binding strength to the same analyte. For example, 50 mM fructose decreased the fluorescence intensity to 38% of the initial intensity for the ARS_5N3CPBA-PPEG8 complex. In the cases of 2CPBA-PPEG8, 3CPBA-PPEG8,

dx.doi.org/10.1021/ja307085h | J. Am. Chem. Soc. 2012, 134, 17620−17627

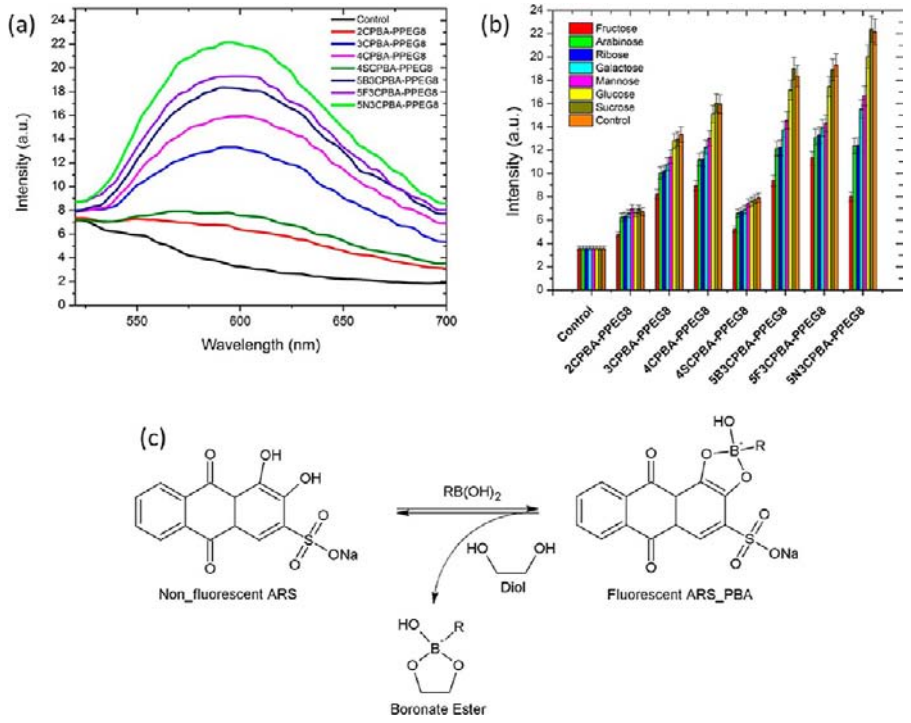

Figure 5. Visible fluorescence from ARS complexed with free PBA-PPEG8 polymer derivatives confirming successful boronic acid conjugation to the PPEG8 scaffold. (a) ARS is originally nonfluorescent but emits upon complexation with the phenyl boronic acid moiety. (b) Subsequent displacement by a panel of various sugars confirms carbohydrate recognition and the relative affinities for each for the functionalized polymer in the absence of the carbon nanotube. The fluorescence intensity is compared at 594 nm. Error bars were compiled from triplicate experiments. (c) Scheme showing competitive binding of a PBA with ARS and a diol. Two hydroxyl groups of ARS can bind to PBA and form a fluorescent ARS−PBA complex. The addition of a diol such as sugar molecules causing a new binding between diol and PBA can disrupts the original equilibrium so that the amount of ARS−PBA complex is decreased resulting in a diminished fluorescence intensity.

4CPBA-PPEG8, 4SCPBA-PPEG8, 5B3CPBA-PPEG8, and 5F3CPBA-PPEG8, the numbers are respectively 70%, 63%, 55%, 65%, 52%, and 62%. Comparison of the results from 2CPBA-PPEG8, 3CPBA-PPEG8, and 4CPBA-PPEG8 indicates that steric effects definitely play an important role for the observed variation of binding strength. Diols can easily bind to para-substituted PBA, while ortho-substituted PBA is the most difficult to bind to. Comparison of the results from 4CPBA-PPEG8 and 4SCPBA-PPEG8 indicates that electron-donating groups such as −NHC(═O)R appear to diminish the binding affinity. Consistent with this observation, a comparison of the results from 3CPBA-PPEG8, 5B3CPBA-PPEG8, 5F3CPBA-PPEG8, and 5N3CPBA-PPEG8 indicates that electron-withdrawing groups such as halogens and nitro groups increase binding via a corresponding reduction in electron density.

Lastly, we examined the nIR fluorescence response of the SWNT upon addition of a panel of saccharides. Our interest is in whether the boronate ion can optically modulate the SWNT fluorescence as we observed earlier in a screening study of surfactant-wrapped SWNT.[11] In addition to common monosaccharides and two disaccharides (sucrose and maltose), we also examined urea as a control for hydrogen-bond disruption, and dopamine which we have reported earlier to be a potent quencher of SWNT emission provided the absorbed phase at the nanotube surface allows for interaction.[9] The results appear as Figure 6. First, it is clear that the PBA attachment is required for sugar recognition as expected, since PPEG8-SWNT has no response except from the dopamine control. Dopamine behaves as a nonspecific quencher due to direct $\pi-\pi$ stacking and electron transfer from the SWNT surface.[9] Thus, dopamine exhibits a response on all polymer−SWNT complexes having accessible surface area. The accessibility of the nanotube surface for all polymers is in agreement with the dielectric model (eq 2) used above (Table 1). Only 4CPBA-PPEG8, 4SCPBA-PPEG8, and 5N3CPBA-PPEG8 possessed starting QY high enough to measure saccharide binding responses, and quite intriguingly, the selectivity exhibited in this assay is distinct from that of the free polymers. For example, in the case of 4CPBA-PPEG8-SWNT, the response selectivity is ribose > arabinose > fructose > glucose, while in the case of 4SCPBA-PPEG8-SWNT, the order is arabinose > xylose > ribose > *N*-acetyl-D-glucosamine > maltose. The case of 5N3CPBA-PPEG8-SWNT, is also distinct as arabinose > ribose > *N*-acetyl-D-galactosamine > mannose. These results highlight the potential to engineer new types of sugar recognition by complexation of PBA with the nanotube surface.

It is worth noting that the most apparent responses are from pentoses, such as arabinose, ribose, and xylose, which are monosaccharides with five carbon atoms. Our hypothesis is that the binding between PBA and pentoses causes a distinct and favorable geometric structure at the SWNT surface compared with the binding of six-membered ring diols. For example, fructose has a much higher affinity for PBA than arabinose and ribose,[45] and our own measurements of the free PBA-functionalized polymers in Figure 5b confirm this. In contrast, when the polymers are adsorbed to the SWNT surface, the selectivity to pentoses is clearly observed. This ability to engineer new types of saccharide binding sites with selectivities that differ from the free polymer forms opens up new possibilities to design sensors for the wide range of other sugar types. Further exploration of the nIR

dx.doi.org/10.1021/ja307085h | *J. Am. Chem. Soc.* 2012, 134, 17620−17627

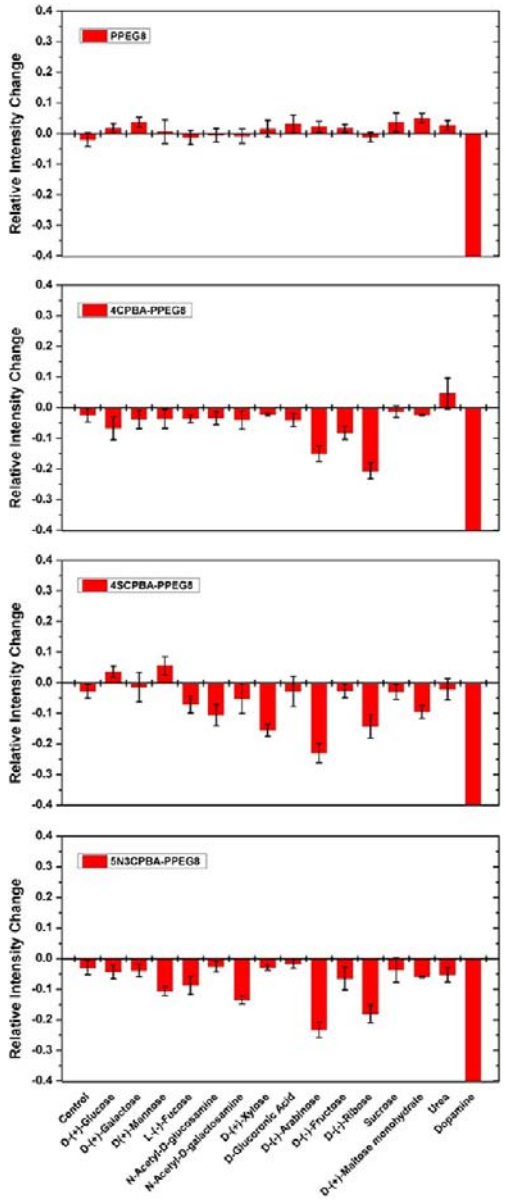

Figure 6. Response of saccharides in different PBA-PPEG8 polymer-dispersed SWNT solutions. All polymer-wrapped SWNT solutions were diluted using PBS buffer to a final SWNT concentration of 2 mg/L. The concentration of SWNT was determined using absorbance at 632 nm with $c = 0.036\ (\mathrm{mg/L})^{-1}\ \mathrm{cm}^{-1}$. All analytes were dissolved in water at 1 M concentration. A quantity of 2 μL of analyte solutions was added to 200 μL SWNT, such that the final analyte concentration was 10 mM. The mixture solution was incubated for 1 h before the nIR fluorescence measurement. The intensity change is calculated on the basis of the fluorescence of SWNT (9, 4). Error bars are given by repeating three times for each measurement. Dopamine completely quenched the fluorescence of SWNTs as a positive control.

fluorescence sensing mechanism is necessary, as the response may come from the following mechanisms: (1) a change of medium polarity near SWNTs, namely solvatochromism; (2) electron transfer due to redox potential change; (3) protons generated by the acid–conjugate base reaction for PBA in water;[46] or (4) the steric effect of a quencher due to conformational, structural, or geometric changes. Although steric effects can play a major role, the variation of the observed selectivity may come from the combined effects of the above mechanisms.

CONCLUSIONS

In summary, we have designed and synthesized a series of PBA-conjugated amphiphilic PEG polymers, examined the interaction of these polymers with SWNTs using different spectroscopies, and finally examined the ability of these polymer–SWNTs to modulate fluorescence emission in response to different saccharides. Comparison of nIR fluorescence of SWNT wrapped by ortho-, meta-, and para-substituted PBA-PPEG8 polymers indicated that the conformational variation has important effects on the quantum yield of SWNTs. We assert that this results from changing dihedral angles between the aromatic ring on PBA and the surface of SWNTs, causing varied strength of $\pi-\pi$ interactions. By measuring photoluminescence excitation–emission profiles, we found that longer-chain hydrocarbons can cause a greater wavelength red-shift in nIR fluorescence of SWNT than shorter-chain hydrocarbons. In addition, compared with E_{11}, the optical transition energy E_{22} is less affected by the wrapping agents, which confirmed our previous observation. By using a fluorophore ARS, the synthesized PBA-PPEG8 polymers demonstrated the same saccharide binding selectivity, namely, fructose > galactose > mannose > glucose > sucrose, for most monosubstituted boronic acids. Furthermore, our results indicated that electron-withdrawing groups such as halogens and nitro groups can help remove the electron density of the system, causing a strong binding between PBA and diols. Last, the examination of nIR fluorescence response of saccharides in different polymer–SWNT solutions demonstrated that the novel signal transfer mechanism can be used to manipulate the binding selectivity of saccharides, which may open an avenue to a new approach to detecting biomolecules which are otherwise difficult to recognize. In brief, our study demonstrates a successful concept design and experimental performance as the first PBA-conjugated polymer–SWNT complexes for saccharide recognition. Furthermore, this idea can be expanded upon, namely by conjugating different recognition groups to the amphiphilic polymers in constructing nanotube optical sensors toward a variety of different applications.

ASSOCIATED CONTENT

Supporting Information

NMR, FT-IR, and UV spectra of PBA and synthesized PBA-PPEG8 polymers. This material is available free of charge via the Internet at http://pubs.acs.org.

AUTHOR INFORMATION

Corresponding Author

*strano@mit.edu

Notes

The authors declare no competing financial interest.

ACKNOWLEDGMENTS

This work is funded by Sanofi-Aventis. We appreciate their financial support.

REFERENCES

(1) Yan, J.; Fang, H.; Wang, B. H. *Med. Res. Rev.* **2005**, *25*, 490.
(2) James, T. D. In *Creative Chemical Sensor Systems*; Topics in Current Chemistry, Schrader, T., Ed.; Springer: New York, Berlin, **2007**; Vol. *277*, p 107.
(3) Jin, S.; Cheng, Y. F.; Reid, S.; Li, M. Y.; Wang, B. H. *Med. Res. Rev.* **2010**, *30*, 171.
(4) Barone, P. W.; Baik, S.; Heller, D. A.; Strano, M. S. *Nat. Mater.* **2005**, *4*, 86.

(5) Heller, D. A.; Baik, S.; Eurell, T. E.; Strano, M. S. *Adv. Mater.* **2005**, *17*, 2793.
(6) Choi, J. H.; Strano, M. S. *Appl. Phys. Lett.* **2007**, 90.
(7) Silvera-Batista, C. A.; Wang, R. K.; Weinberg, P.; Ziegler, K. J. *Phys. Chem. Chem. Phys.* **2010**, *12*, 6990.
(8) Shoda, M.; Bandow, S.; Maruyama, Y.; Iijima, S. *J. Phys. Chem. C* **2009**, *113*, 6033.
(9) Zhang, J. Q.; Boghossian, A. A.; Barone, P. W.; Rwei, A.; Kim, J. H.; Lin, D. H.; Heller, D. A.; Hilmer, A. J.; Nair, N.; Reuel, N. F.; Strano, M. S. *J. Am. Chem. Soc.* **2011**, *133*, 567.
(10) Satishkumar, B. C.; Brown, L. O.; Gao, Y.; Wang, C.-C.; Wang, H.-L.; Doorn, S. K. *Nat. Nano* **2007**, *2*, 560.
(11) Yum, K.; Ahn, J. H.; McNicholas, T. P.; Barone, P. W.; Mu, B.; Kim, J. H.; Jain, R. M.; Strano, M. S. *ACS Nano* **2012**, *6*, 819.
(12) Barone, P. W.; Strano, M. S. *Angew. Chem., Int. Ed.* **2006**, *45*, 8138.
(13) Reuel, N. F.; Ahn, J. H.; Kim, J. H.; Zhang, J. Q.; Boghossian, A. A.; Mahal, L. K.; Strano, M. S. *J. Am. Chem. Soc.* **2011**, *133*, 17923.
(14) Heller, D. A.; Pratt, G. W.; Zhang, J. Q.; Nair, N.; Hansborough, A. J.; Boghossian, A. A.; Reuel, N. F.; Barone, P. W.; Strano, M. S. *Proc. Natl. Acad. Sci. U.S.A.* **2011**, *108*, 8544.
(15) Kim, J. H.; Patra, C. R.; Arkalgud, J. R.; Boghossian, A. A.; Zhang, J. Q.; Han, J. H.; Reuel, N. F.; Ahn, J. H.; Mukhopadhyay, D.; Strano, M. S. *ACS Nano* **2011**, *5*, 7848.
(16) Ahn, J. H.; Kim, J. H.; Reuel, N. F.; Barone, P. W.; Boghossian, A. A.; Zhang, J. Q.; Yoon, H.; Chang, A. C.; Hilmer, A. J.; Strano, M. S. *Nano Lett.* **2011**, *11*, 2743.
(17) Szleifer, I.; Yerushalmi-Rozen, R. *Polymer* **2005**, *46*, 7803.
(18) Wong, M.; Paramsothy, M.; Xu, X. J.; Ren, Y.; Li, S.; Liao, K. *Polymer* **2003**, *44*, 7757.
(19) Chen, R. J.; Zhang, Y.; Wang, D.; Dai, H. *J. Am. Chem. Soc.* **2001**, *123*, 3838.
(20) Islam, M. F.; Rojas, E.; Bergey, D. M.; Johnson, A. T.; Yodh, A. G. *Nano Lett.* **2003**, *3*, 269.
(21) Rasheed, A.; Dadmun, M. D.; Ivanov, I.; Britt, P. F.; Geohegan, D. B. *Chem. Mater.* **2006**, *18*, 3513.
(22) Boghossian, A. A.; Zhang, J. Q.; Barone, P. W.; Reuel, N. F.; Kim, J. H.; Heller, D. A.; Ahn, J. H.; Hilmer, A. J.; Rwei, A.; Arkalgud, J. R.; Zhang, C. T.; Strano, M. S. *ChemSusChem* **2011**, *4*, 848.
(23) Cambre, J. N.; Sumerlin, B. S. *Polymer* **2011**, *52*, 4631.
(24) Jäkle, F. *Chem. Rev.* **2010**, *110*, 3985.
(25) Vainio, P.; Virtanen, J. A.; Kinnunen, P. K. J. *Biochim. Biophys. Acta* **1982**, *711*, 386.
(26) Jay, J. I.; Shukair, S.; Langheinrich, K.; Hanson, M. C.; Cianci, G. C.; Johnson, T. J.; Clark, M. R.; Hope, T. J.; Kiser, P. F. *Adv. Funct. Mater.* **2009**, *19*, 2969.
(27) Wang, B.; Ma, R.; Liu, G.; Li, Y.; Liu, X.; An, Y.; Shi, L. *Langmuir* **2009**, *25*, 12522.
(28) Bench, B. J.; Johnson, R.; Hamilton, C.; Gooch, J.; Wright, J. R. *J. Colloid Interface Sci.* **2004**, *270*, 315.
(29) Kim, K. T.; Cornelissen, J. J. L. M.; Nolte, R. J. M.; van Hest, J. C. M. *J. Am. Chem. Soc.* **2009**, *131*, 13908.
(30) Gao, S.; Wang, W.; Wang, B. *Bioorg. Chem.* **2001**, *29*, 308.
(31) Shoji, E.; Freund, M. S. *J. Am. Chem. Soc.* **2002**, *124*, 12486.
(32) Elbert, D. L.; Hubbell, J. A. *Annu. Rev. Mater. Sci.* **1996**, *26*, 365.
(33) Zhao, J.; Lu, J. P.; Han, J.; Yang, C.-K. *Appl. Phys. Lett.* **2003**, *82*, 3746.
(34) Star, A.; Han, T.-R.; Gabriel, J.-C. P.; Bradley, K.; Grüner, G. *Nano Lett.* **2003**, *3*, 1421.
(35) Alldredge, E. S.; Badescu, S. C.; Bajwa, N.; Perkins, F. K.; Snow, E. S.; Reinecke, T. L. *Phys. Rev. B* **2010**, 82.
(36) Woods, L. M.; Bădescu, Ş. C.; Reinecke, T. L. *Phys. Rev. B* **2007**, *75*, 155415.
(37) Hung, W.-C.; Elias, G.; Wai, C. M. *ChemPhysChem* **2010**, *11*, 3439.
(38) Moore, V. C.; Strano, M. S.; Haroz, E. H.; Hauge, R. H.; Smalley, R. E.; Schmidt, J.; Talmon, Y. *Nano Lett.* **2003**, *3*, 1379.
(39) Yang, M. J.; Koutsos, V.; Zaiser, M. *J. Phys. Chem. B* **2005**, *109*, 10009.
(40) Xu, Z.; Yang, X.; Yang, Z. *Nano Lett.* **2010**, *10*, 985.
(41) Almgren, M.; Swarup, S. *J. Colloid Interface Sci.* **1983**, *91*, 256.
(42) Duan, W. H.; Wang, Q.; Collins, F. *Chem. Sci.* **2011**, *2*, 1407.
(43) Tummala, N. R.; Striolo, A. *ACS Nano* **2009**, *3*, 595.
(44) Springsteen, G.; Wang, B. H. *Chem. Commun.* **2001**, 1608.
(45) James, T. D.; Phillips, M. D.; Shinkai, S. *Boronic Acids in Saccharide Recognition*; RSC Publishing: Cambridge, U.K., 2006.
(46) Cognet, L.; Tsyboulski, D. A.; Rocha, J.-D. R.; Doyle, C. D.; Tour, J. M.; Weisman, R. B. *Science* **2007**, *316*, 1465.